Energy Proceedings
Vol 40, 2024
ISSN 2004-2965

Heating Performance Improvement on an R290 Vapor-Injection Heat Pump System With Waste Heat Recovery for Electric Vehicles

Yunchun Yang [1,2], Tianyang Yang [1,2], Wencong Shao [1,2], Huiming Zou [1,2], Changqing Tian [1,2]*

1 Technical Institute of Physics and Chemistry, Key Laboratory of Technology on Space Energy Conversion and Key Laboratory of Cryogenics, CAS, Beijing 100190, China
2 University of Chinese Academy of Sciences, Beijing 100049, China
*Corresponding Author: chqtian@mail.ipc.ac.cn

ABSTRACT

Achieving environmental governance and energy poverty alleviation requires high-efficiency and environmental-friendly thermal management systems for electric vehicles. This study developed and tested an integrated R290 (propane) vapor-injection (INJ) heat pump system with waste heat recovery in a cold climate. Dual secondary loops are adopted considering the flammability of the R290 refrigerant. Experimental results reveal that the INJ system outperforms the basic (BAS) system by 12.1% in coefficient of performance (COP) and 36.3% in heating capacity at −20 °C/20 °C (out-cabin/in-cabin) ambient temperature. The INJ mode with 1 kW waste heat recovery can provide a 29.8% improvement in heat capacity and a 7.4% increase in COP compared to that with no waste heat at −20 °C/20 °C. This study provides experimental support for achieving efficient operation of automotive heat pump systems under a wide operation temperature range.

Keywords: electric vehicles, thermal system, heat pump, R290, vapor injection, secondary loop

NONMENCLATURE

Abbreviations	
BAS	Basic
COP	Coefficient of performance
HX	Heat exchanger
IHX	Internal heat exchanger
INJ	Vapor-injection
Symbols	
c_p	Specific heat, J/(kg·K)
m	Mass flow rate, kg/s
Q	Heating capacity, W
t	Temperature, °C
T	Temperature, °C
W	Compressor input power, W
Subscripts	
a	Air
in	Inlet
out	Outlet
s	Supply
w	Water

1. INTRODUCTION

The automotive thermal system is a key technology of new energy vehicles, and the performance of traditional heat pumps limits vehicle driving range as well as working temperature range. Vapor injection technology is an effective approach to achieving high-efficient heat pump systems working in a wide temperature range. Qin et al. [1] designed a heat pump system with refrigerant injection, and results showed that the heating capacity of the INJ system could be increased up to 31%. An economizer or a flash tank is normally used in vapor-injection (INJ) heat pump systems. For the upstream injection, downstream injection, and flash tank vapor injection systems, the COP can be increased by 24.2%, 16.9%, and 92.3%, respectively [2]. Han et al. [3] experimentally investigated an INJ heat pump system with waste heat recovery for electric buses, and found that heating capacity and COP improvements of the heat pump with 6 kW waste heat recovery were 5.12% and 2.56%, respectively. Yang [4] conducted experiments on an INJ CO_2 heat pump system from −30°C to 50°C, showing that the COP and heating capacity of the INJ system were increased by 45.5% and 75.7% at −30°C/20°C.

Traditional HFCs refrigerants like R134a are about to be replaced due to the demand of the Kigali Amendment. R290, a natural gas with ODP=0 and low GWP, is a potential alternative to refrigerants. Gaurav and Kumar [5] found that R290 had the highest relative COP and exergy efficiency compared to multiple R134a alternatives. Huang et al. [6] experimentally investigated the performances of R290 and CO_2 systems, concluding that the R290 system had a good heating performance

This is a paper for 15th International Conference on Applied Energy (ICAE2023), Dec. 3-7, 2023, Doha, Qatar.

and had 5.77% larger cooling capacity than the CO_2 system.

Although R290 has both good heating and cooling performances, the flammability limits its use in the field of automotive thermal systems. Zhang et al. [7] analyzed R290 leakage characteristics and distributions and provided some solutions that applying secondary loops was one of the most effective methods. It could easily recover waste heat produced by batteries and motors [8], as well as showed excellent anti-frost performance due to more uniform distribution in heat exchangers [9]. Wang et al. [10] experimentally investigated the performance of a R290 INJ heat pump with secondary loops, and analyzed the influences of vapor injection, ambient temperature, compressor speed, etc. The results showed that the INJ system had 25.0% higher heating capacity and 15.3% higher COP compared to the basic (BAS) system under −20 °C ambient temperature and 6750 rpm compressor speed. The PTC heater is not necessary if adopting waste heat recovery.

In this study, an integrated INJ heat pump system is designed, with dual secondary loops performing heat exchange with in-cabin and out-cabin HXs. The refrigerant circulation is sealed by a double-layer tank which also serves as an expansion tank, so as to prevent leakage to the outside. The heating performances of BAS and INJ systems are experimentally investigated under a cold climate at 0 °C and −20 °C. The waste heat recovery technology and secondary loop loss are evaluated as well. This study would provide experimental support for the improvement and application of R290 heat pump systems.

2. EXPERIMENTAL SETUP AND PERFORMANCE ANALYSIS

2.1 System description

The test bench of the proposed R290 INJ heat pump system is built up as demonstrated in *Fig. 1* and *Fig. 2*, including a refrigerant cycle and dual secondary loops. The INJ system with an economizer is adopted in the refrigerant cycle, and a valve is added to accomplish the function of the no INJ (i.e., BAS) mode. The secondary loops involve two four-way valves, so as to switch between cooling and heating modes. The details of main components are listed in Table 1.

Several pressure sensors (± 0.5% uncertainties), temperature sensors (± 0.1 °C uncertainties), and mass flow meters (± 0.5%) are also set in the bench in order to obtain refrigerant status, as shown in *Fig. 1*. The air-side parameters can be directly obtained from the enthalpy difference laboratory, in which the measurement uncertainties are ± 0.1 °C for air temperature, ± 1% for air flow rate, and ± 0.2% for input power.

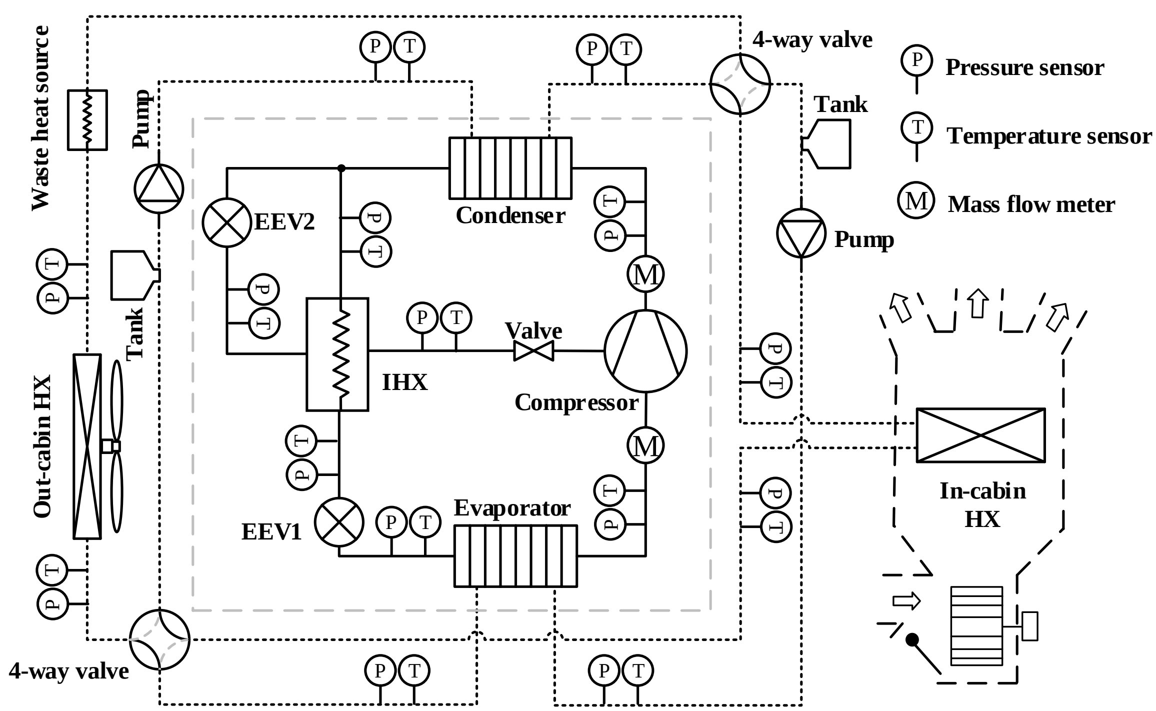

Fig. 1 Schematic diagram of a R290 Vapor-injection Heat Pump System Experimental bench

Fig. 2 Experimental bench

Table 1 Component Information

Components	Specifications
Compressor	34cc Scroll compressor
Condenser	24 channel Plate HX
	153 mm × 69 mm
Evaporator	18 channel Plate HX
	153 mm × 69 mm
IHX	30 channel Plate HX
	88 mm × 64 mm
EEV 1&2	0–500 steps
In-cabin HX	2 louver-fin flat-tube HXs in series
	20.5 mm × 18 mm
Out-cabin HX	Louver-fin flat-tube HX
	710 mm × 44 mm

The experiments are conducted at −20 °C and 0 °C ambient temperatures, and the in-cabin temperature is maintained at 20 °C. A fixed air flow rate of 4000 m^3/h and 500 m^3/h are provided to the out-cabin HX and in-cabin HXs, respectively. An identical refrigerant mass of 260g and an identical compressor speed of 3000 rpm are held in different systems in all tests. EEV's openings of different system configurations are also fixed at −20 °C and 0 °C, respectively. The waste heat amount includes 1 kW and 2 kW.

2.2 *Performance analysis*

Typical BAS and INJ heat pump cycles are exhibited in *Fig. 3*. The BAS cycle flow is 1–10–3–11–1. The INJ cycle includes a main branch (1–8–9–2–3–4–5–1) and a vapor-injection branch (7–9–2–3–6–7). As it is difficult to determine the process inside the compressor, the dashed lines 7–2 (from vapor-injection state to discharge state) and 1–2 (from suction state to discharge state) are used to represent processes inside the compressor. The following assumptions in throttling processes are also adopted in this paper: h_3=h_{11}, h_3=h_6, h_4=h_5.

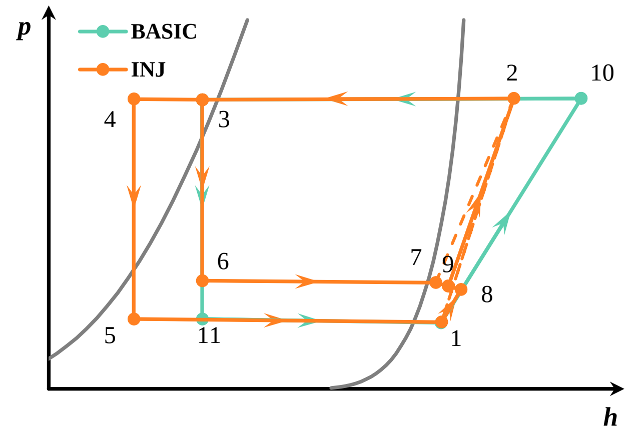

Fig. 3 P-h diagram of basic and vapor-injection cycle

The heating capacity can be measured from the water side and air side:

$$Q_w = \dot{m}_w c_{p,w} (t_{w,out} - t_{w,in}) \quad (1)$$

$$Q_a = \dot{m}_a c_{p,a} (t_{a,out} - t_{a,in}) \quad (2)$$

A heating capacity loss can be defined as:

$$\triangle Q = Q_w - Q_a \quad (3)$$

The COP of water side and air side can be calculated as follows:

$$COP_w = Q_w / W \quad (4)$$

$$COP_a = Q_a / W \quad (5)$$

A COP loss can be defined as:

$$\mathrm{d}COP = (COP_w - COP_a) / COP_w \quad (6)$$

Calculating based on Moffat's equations [11], the maximum uncertainties of heating capacity and COP are ± 3.9% and ± 4.2%, respectively.

3. RESULTS AND DISCUSSIONS

As demonstrated in *Fig. 4*, the INJ system improves COP from 1.85 to 2.00, which is 8.1% at 0 °C compared to the BAS system, and this increase goes up to 12.1% when ambient temperature is −20 °C (from 1.32 to 1.48). Applying waste heat recovery technology can increase COP at a cold climate of −20 °C; particularly, the INJ system with 1 kW waste heat recovery (1.59) has 7.4% better COP compared to the INJ system with no waste heat recovery (1.48). At 0 °C, the COPs of the INJ system with 0, 1, and 2 kW waste heat recovery are almost identical. The COP loss (dCOP) caused by secondary loops fluctuates from 8.7% to 15.1%.

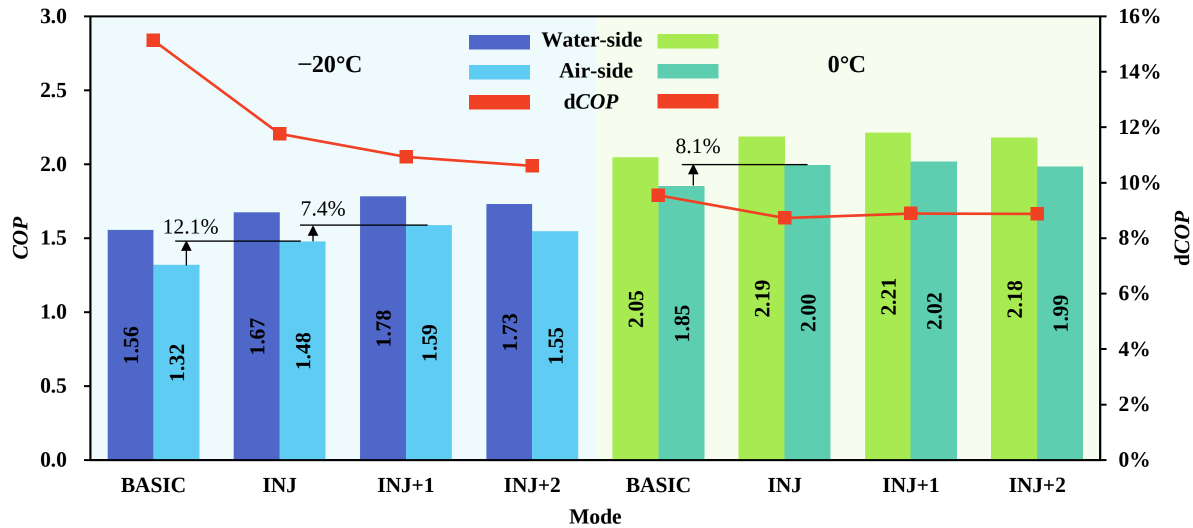

Fig. 4 COP and dCOP of different systems at−20 °C and 0 °C ambient temperature

The vapor injection technology can significantly rise heating capacity, particularly in an extremely cold climate. *Fig.5* illustrates that the INJ system provides 18.2% more heating capacity at 0 °C and 36.3% more at −20 °C, compared to the BAS system. The INJ system with 1 kW waste heat recovery increases heating capacity by 29.8% and 12.0%, and the INJ system with 2 kW waste heat recovery increases heating capacity by 8.4% and 8.3%, at −20 °C and 0 °C, respectively. The heating capacity loss (ΔQ) caused by secondary loops ranges from 279 W to 404 W.

Similar to the heating capacity, the compressor power also increases from the BAS system to the INJ system with waste heat recovery. It leads to a situation that too much waste heat recovery at the evaporator side will rather lower system COP as shown in *Fig. 4*.

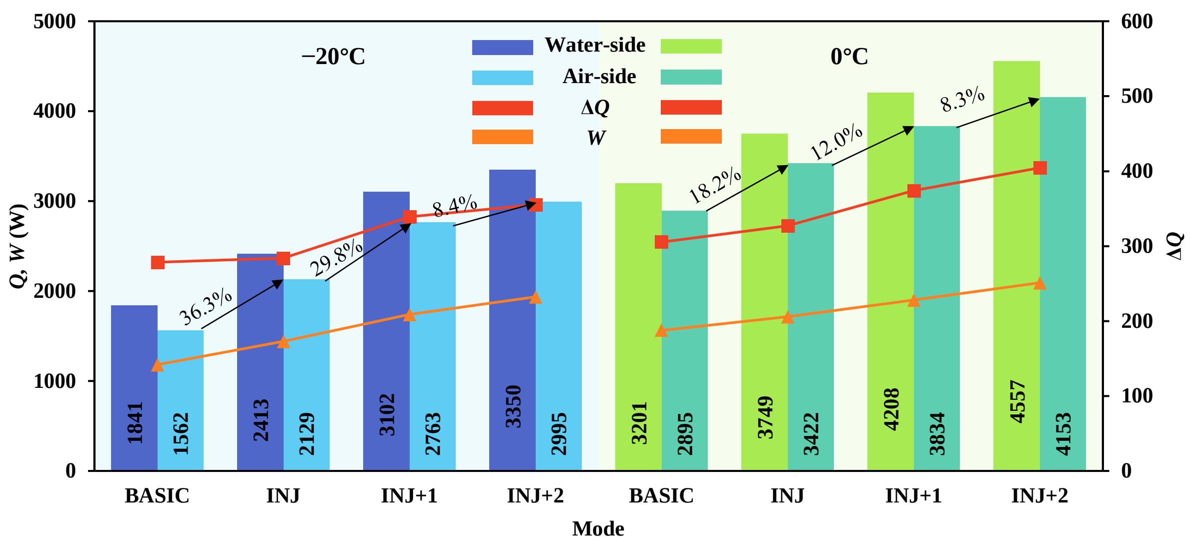

Fig. 5 Heating capacity (Q), compressor power (W) and ΔQ of different systems at −20 °C and 0 °C ambient temperature

Fig.6 shows the supply air temperature of different heat pump systems and the supply air temperature loss (ΔT_s) caused by secondary loops. All systems can provide supply air temperature higher than 37 °C when ambient temperature is 0 °C. The INJ system provides 3.2 °C higher supply air temperature than the BAS system does, and the INJ system with 2 kW waste heat recovery provides the highest supply air temperature of 44.8 °C. At −20 °C ambient temperature, the INJ system provides 32.7 °C supply air temperature which is 3.4 °C higher than that of the BAS system. The INJ system with 1 kW and 2 kW waste heat recovery provides 36.6 °C and 37.9 °C air, respectively. The temperature decreases from the water side to the air side ranges from 4.3 °C to 7.8 °C at −20 °C ambient temperature, and from 7.3 °C to 10.5°C at 0 °C.

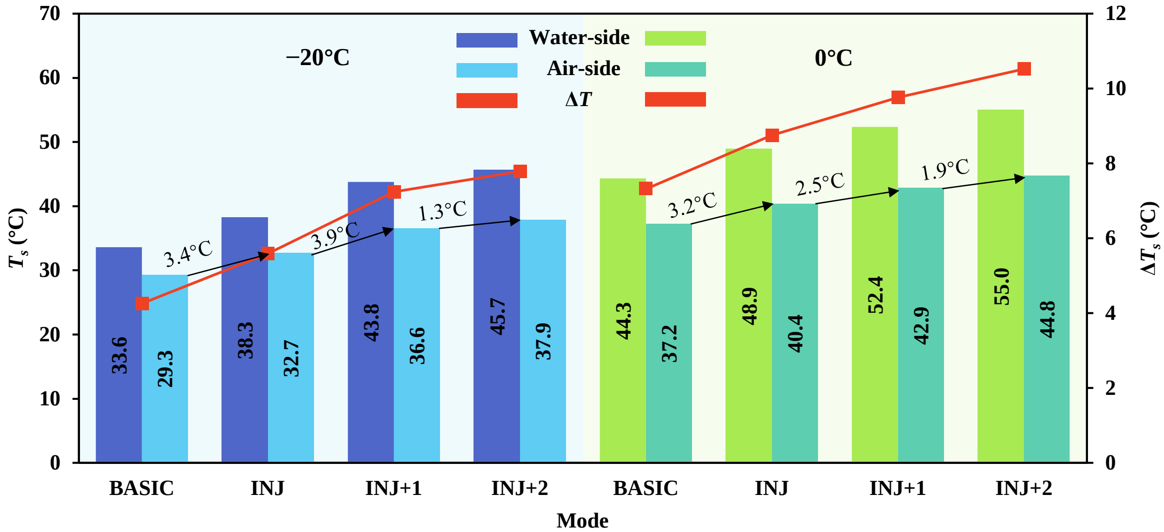

Fig. 6 Supply water/air temperature (T) and ΔT of different systems at −20 °C and 0 °C ambient temperature

More detailed system characteristics can be obtained from *Fig. 7*. At −20 °C ambient temperature, the discharge temperature of the BAS system is up to 134.4 °C which is above the compressor's upper limit of 125 °C and may damage the compressor, while the INJ system has obviously lower discharge temperature of 99.64 °C. The waste heat recovery significantly rises injection pressure and discharge pressure. At 0 °C, the injection pressure of the INJ systems with 0, 1, 2 kW are 0.580, 0.656, 0.725 MPa, and the discharge pressure of the INJ systems with 0, 1, 2 kW are 1.666, 1.797, 1,916 MPa.

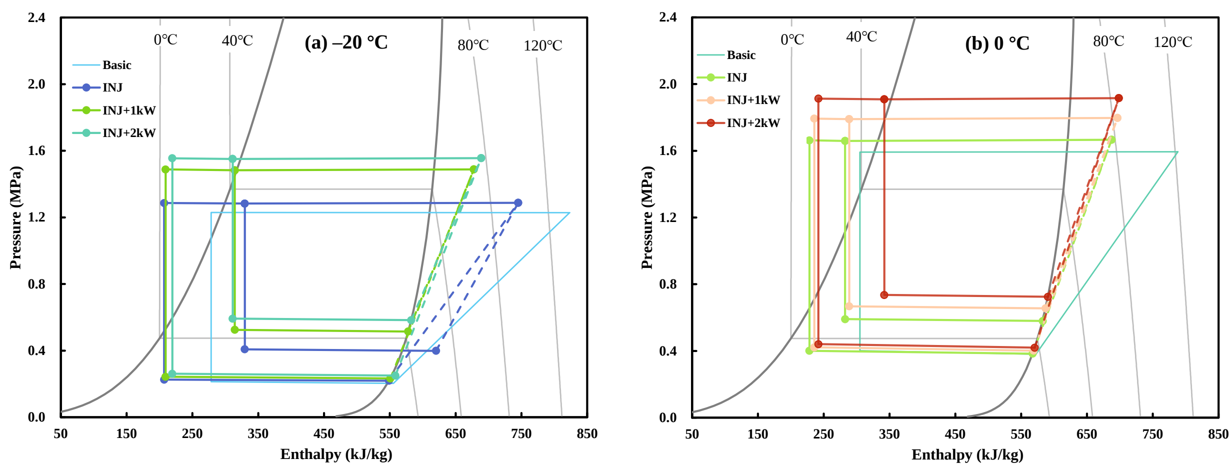

Fig. 7 P-h diagram of different systems at −20 °C (a) and 0 °C (b) ambient temperature

4. CONCLUSIONS

This study proposed an integrated vapor-injection (INJ) system with dual secondary loops, examined the heating performance of INJ and basic (BAS) systems in a cold climate, and analyzed system characteristics of waste heat recovery and secondary loop loss. The main conclusions can be summarized as follows:

(1) The COP and heating capacity of the INJ system are increased by 12.1% and 36.3% at −20 °C/20 °C, 8.1% and 18.2% at 0 °C/20 °C, respectively, compared to the BAS system.

(2) The INJ system with 1 kW waste heat recovery performs best that its COP is 1.59 at −20 °C/20 °C, while waste heat recovery does not obviously increase COP at 0 °C/20 °C.

(3) The discharge temperature of the INJ system is 99.64 °C which is obviously lower than that of the BAS system (134.4 °C) at −20 °C/20 °C. The heating performance loss caused by secondary loops is 10.6% on average.

ACKNOWLEDGEMENT

This research was financially supported by the Special Fund Project of High-tech Industrialization for

Science and Technology Cooperation between Jilin Province and the Chinese Academy of Sciences (No. 2021SYHZ0017).

REFERENCE

[1] F. Qin, Q. Xue, G.M. Albarracin Velez, G. Zhang, H. Zou, C. Tian, Experimental investigation on heating performance of heat pump for electric vehicles at −20°C ambient temperature, Energy Conversion and Management. 102 (2015) 39–49. https://doi.org/10.1016/j.enconman.2015.01.024.

[2] K. Li, J. Ma, B. Zhang, L. Su, N. Liu, H. Zhang, B. Dou, Q. He, X. Zhou, R. Tu, Experimental study on low temperature heating performance of different vapor injection heat pump systems equipped with a flash tank and economizers for electric vehicle, Applied Thermal Engineering. 227 (2023) 120428. https://doi.org/10.1016/j.applthermaleng.2023.120428.

[3] X. Han, H. Zou, J. Wu, C. Tian, M. Tang, G. Huang, Investigation on the heating performance of the heat pump with waste heat recovery for the electric bus, Renewable Energy. 152 (2020) 835–848. https://doi.org/10.1016/j.renene.2020.01.075.

[4] T. Yang, H. Zou, M. Tang, C. Tian, Y. Yan, Experimental performance of a vapor-injection CO2 heat pump system for electric vehicles in −30 °C to 50 °C range, Applied Thermal Engineering. 217 (2022) 119149. https://doi.org/10.1016/j.applthermaleng.2022.119149.

[5] Gaurav, R. Kumar, Computational energy and exergy analysis of R134a, R1234yf, R1234ze and their mixtures in vapour compression system, Ain Shams Engineering Journal. 9 (2018) 3229–3237. https://doi.org/10.1016/j.asej.2018.01.002.

[6] Y. Huang, X. Wu, J. Jing, Research on the electric vehicle heat pump air conditioning system based on R290 refrigerant, Energy Reports. 8 (2022) 447–455. https://doi.org/10.1016/j.egyr.2022.05.112.

[7] Y. Zhang, C. Liu, T. Wang, L. Pan, W. Li, J. Shi, J. Chen, Leakage analysis and concentration distribution of flammable refrigerant R290 in the automobile air conditioner system, International Journal of Refrigeration. 110 (2020) 286–294. https://doi.org/10.1016/j.ijrefrig.2019.11.001.

[8] Z. Tian, W. Gan, X. Zhang, B. Gu, L. Yang, Investigation on an integrated thermal management system with battery cooling and motor waste heat recovery for electric vehicle, Applied Thermal Engineering. 136 (2018) 16–27. https://doi.org/10.1016/j.applthermaleng.2018.02.093.

[9] W. Li, Y. Liu, R. Liu, D. Wang, J. Shi, Z. Yu, L. Cheng, J. Chen, Performance evaluation of secondary loop low-temperature heat pump system for frost prevention in electric vehicles, Applied Thermal Engineering. 182 (2021) 115615. https://doi.org/10.1016/j.applthermaleng.2020.115615.

[10] H. Wang, Z. Ji, C. Wang, Z. Zhu, Y. Wang, H. Lin, Experimental study of propane heat pump system with secondary loop and vapor injection for electric vehicle application in cold climate, Applied Thermal Engineering. 217 (2022) 119196. https://doi.org/10.1016/j.applthermaleng.2022.119196.

[11] R.J. Moffat, Describing the uncertainties in experimental results, Experimental Thermal and Fluid Science. 1 (1988) 3–17. https://doi.org/10.1016/0894-1777(88)90043-X.